LBL-21820

Presented at the Society of Photo-optical
Instrumentation Engineers Conference,
San Diego, CA, August 18–20, 1986, and to
be published in the Proceedings

Overview of Advances in Light Sources

D.D. Hollister

June 1986

Prepared for the U.S. Department of Energy under Contract DE-AC03-76SF00098

Presented at the Conference of the Society of Photo-optical Instrumentation Engineers, San Diego, CA, August 18-20, 1986.

Overview of advances in light sources

Donald D. Hollister

Lighting Systems Research, Lawrence Berkeley Laboratory, University of California, Berkeley, California 94720

Abstract

Current efforts at the Lawrence Berkeley Laboratory to improve the operational efficiency of fluorescent lamps are based upon novel techniques intended to reduce internal resonance radiative transport losses. Such losses have been associated with "entrapment" of resonance radiation in the optically thick positive column of the mercury vapor discharge. Two promising techniques for entrapment reduction are provided respectively to selective mercury isotope enrichment and by the broadening of the hyperfine structure (hfs) of the resonance line λ2537 via the Zeeman effect. These techniques have, thus far, led to fluorescent lamp UV production efficiency enhancements, respectively of about 6.8% and 7%.

Additional efforts to improve HID sources are in progress. Interesting metallic halides have been combined with electrodeless arc technology to produce a laboratory discharge system operating with an efficacy exceeding 170 lumens per watt, and a color rendering index (CRI) of 52.

Introduction

During recent years the Lighting Group at Lawrence Berkeley Laboratory (LBL), under the auspices of the Department of Energy, has been studying novel technologies and methods for enhancing the efficacies of various lighting systems. These studies include in-house theoretical and experimental research and outside research performed under subcontract by industrial research groups. One of our purposes is to examine and encourage development of commercially "high risk" concepts which eventually, if properly nurtured, may yield highly efficient energy conserving technology for the general public.

This discussion will outline two current developments in flourescent lighting (i.e., the low pressure mercury discharge) and interesting results toward the development of an efficient electrodeless HID source.

Advances in fluorescent lighting, background

An abbreviated energy level diagram for HgI is presented in Fig. (1), where the resonance transition between the 6^3P_1 state and ground is of major interest. This transition yields the intense spectral line at λ2537 that is converted by phosphors at the wall of a fluorescent lamp into visible light. The natural lifetime of this state is about 1.2×10^{-7} seconds[1] and at a sufficiently low mercury vapor pressure this equals the residence time in the discharge of a typical photon at λ2537. As the mercury density increases, the resonance photon undergoes an increasing number of absorptions and re-emissions in the discharge vapor, and at the mercury density of an operating fluorescent lamp ($\simeq 10^{14}$ cm^{-3}) the number of such absorptions and subsequent reemissions has increased to such an extent that the photon residence time has become several hundred times as great as the natural lifetime of the $^3P_1$ state. This phenomenon is called "imprisonment" of the resonance radiation.[2] The theory of imprisonment and its effects is relatively well developed.[3-6] When imprisonment is significant in a mercury discharge it has been found that the $^3P_1$ state is significantly depopulated by collisions of the second kind into the companion levels $^3P_0$ and $^3P_2$. Selection rule constraints do not allow the radiative de-excitation of these levels to ground so once they are occupied, they remain occupied until their energy is removed by a suitable non-radiative process, a collision with the wall or another particle, for example.

The resonance "line" at λ2537 actually consists of ten individual components and has a combined spectral width of about 0.05 Å.[7] This hyperfine structure (hfs) results from the mass differences among the seven stable mercury isotopes and the fact that two of the isotopes have non-zero spins. Because of spectral overlap the ten components combine to form five composite lines, as shown in Fig. (2), where the contribution from ^{196}Hg is negligible because of this isotope's scarcity.

Acknowledgement. This work was supported by the Assistant Secretary for Conservation and Renewable Energy, Office of Building Energy Research and Development, Buildings Equipment Division of the U.S. Department of Energy under Contract No. DE-AC03-76SF00098.

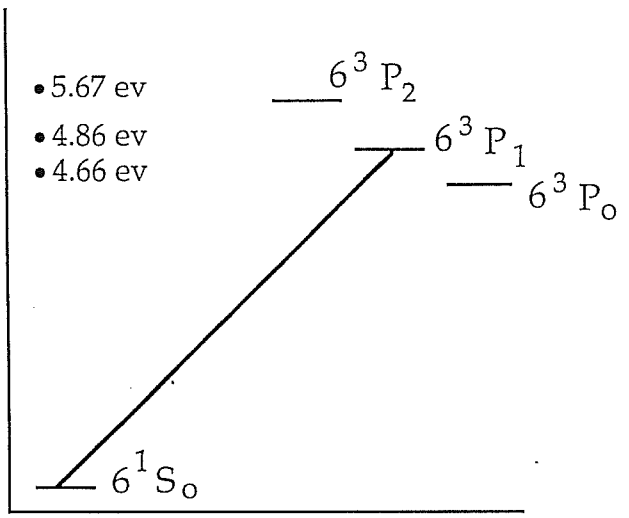

Figure 1. Abbreviated energy level diagram of HgI.

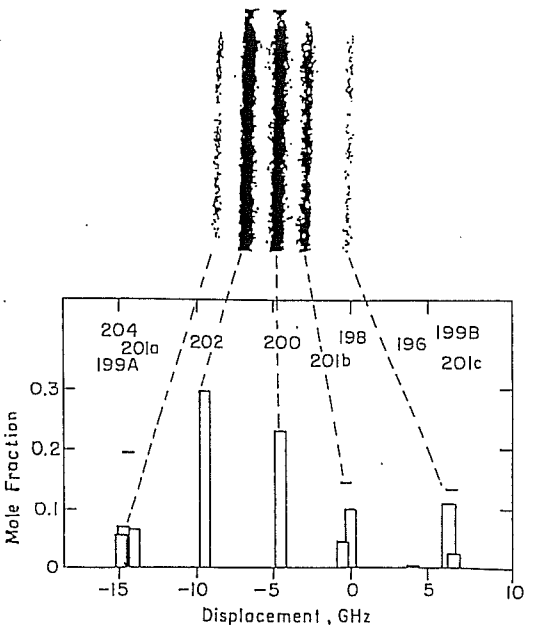

Figure 2. Hyperfine structure of HgI resonance line λ2537.

Early studies of resonance radiation imprisonment[2,8,9] in mercury vapor has given us a basic understanding of the correlation between the extent of imprisonment and the persistence time of resonance radiation. Holstein[3,4] described the imprisonment phenomenon and suggested the existence of a strong relationship between the persistence of imprisonment resonance radiation in a gas and the line shape of radiation. Specifically, because of the hyperfine structure of the natural mercury resonance line, it was believed that the persistence time of resonance radiation associated with a pure isotope having no hfs would have a value roughly five-to-six times as large as that of natural mercury at an equal vapor pressure. Careful measurements of this time were made[3] in natural mercury, and repeated in nearly pure ^{198}Hg vapor. It was found that, for equal number densities, the persistence time of resonance radiation in the isotope is indeed five-to-six times that observed in natural mercury.[10] Additionally, it was determined that, for a sufficiently large number density, trace amounts of ^{199}Hg and ^{200}Hg in the otherwise pure ^{198}Hg enabled otherwise imprisoned resonance radiation from ^{198}Hg to escape via collisions of the second kind between the main isotope and the "impurity" isotopes, thereby lowering the persistence time from the value predicted by theory and hence, increasing the efficiency of UV production.

The spectral locations and related data of the ten hfs components of λ2537 are given in Table I for several units of measure. Comparison of these values with the spectrum of Fig. (2) indicates that the resolvable spectrum of mercury consists of five lines roughly equally spaced with a total line width of about 50 mÅ. If the intensity of each line was made equal, wouldn't the discharge UV production efficiency be optimized?

If each isotope emission spectrum consisted of only one 2537 Å line, one method of resonance radiation enhancement would be to provide equal amounts of each isotope in the mercury discharge. If this were the case, each specie's number density would be equal to that of any other specie (their temperatures are equal), the processes of emission, absorption, imprisonment and loss will be the same for each specie, and the production of resonance radiation by the individual isotopes would be expected to peak at a common cold-spot temperature. However, the isotopes of 199 and 201 AMU have nonzero spins and between them produce five lines, all of which overlap one or more lines of the other isotopes. Since such overlapping is known to promote resonance radiation collisional losses, the above blend must be modified. Rather than blending isotopes to provide equal isotopic amounts, the blend should provide for equal intensities of the resultant hyperfine components.

Another approach would be to increase the number of hyperfine components in the natural mercury blend.[11] In this method ^{196}Hg, initially present only to the extent of 0.14% in natural mercury, is enriched thirty or more fold to add a sixth component to the mercury hfs.

Table 1

line	% Total*	$\Delta\bar{\nu}$ (K=$10^{-3}cm^{-1}$)**	λ (Å)+	$\Delta\lambda$ (mÅ)	$\Delta\nu$ (GH_3)
199A	5.48	-0.51399	2536.5393	+0.0330	-15.376
204	6.85	-0.51077	2536.5391	+0.0328	-15.283
201a	6.84	-0.48896	2536.5377	+0.0314	-14.631
202	29.27	-0.33696	2536.5277	+0.0216	-10.065
200	23.77	-0.16029	2536.5166	+0.0103	-4.799
201b	4.57	-0.02256	2536.5077	+0.0014	-0.652
198	9.89	0	2536.5063	0	0
199B	10.96	+0.22440	2536.4918	-0.0145	+6.757
201C	2.28	+0.22923	2536.4915	-0.0148	+6.896
196	0.14		(2536.4969)	(-0.0094)	(+4.265)
(1)	(3)	(6)	(2)	(4)	(5)

*Mitchell, A. and Zemansky, M., Resonance Radiation and Excited Atoms, 2nd Impression Cambridge University Press, Cambridge, 1961.
**Walter G. Schwertzer, Jr., J. Opt. Soc. Amer. 53, 1055 (1963).
+The reference wavelengths for ^{198}Hg and ^{202}Hg are taken from H.M. Grosswhite, Editor, Section 7, AIP Handbook, McGraw Hill Book Co., New York Ed. 3, (1972), Table 7e-7, pg. 7-93.

A third approach is suggested by a recent[12] variational calculation of the radiant emittance of a mercury-argon discharge. In this method the amount of resonance radiation leaving the discharge is regulated by an inter-line exchange of photons in the overlapping wings of adjacent hfs components. Enhancement of resonance radiation emittance is effected by broadening the regions of overlap. Employing the Zeeman effect, the predicted UV emittance is maximized when the Zeeman line width is of the order of 1.7 Doppler widths. In those cases where the overlapping line widths are determined by isotopic content, for blends of natural mercury with ^{201}Hg the predicted emittance is maximum when the total ^{201}Hg enrichment is about 40%.

Advances in fluorescent lighting, recent results

Isotope blending studies currently are being performed by GTE and LBL.

The GTE investigation reports[13] a significant 6.8% improvement in UV output per arc watt with 2.6% ^{196}Hg in a F40 T/12 quartz discharge tube, in good agreement with total light output integrating sphere measurements when end losses are taken into account. In these measurements both cold spot temperature and Hg isotopic distributions (i.e., the ^{196}Hg content) were varied. The added isotope was contained in internally located ampules which were sequentially broken. All measurements were done in a single lamp, thus avoiding possible lamp-to-lamp variation. When all data had been collected the lamp mercury was analyzed via mass spectrometry to determine the isotopic composition.

The data appearing below were obtained for an arc current of 430 ma with the lamp operating off of a standard rapid start reference ballast. Both U.V. output and U.V. output per arc watt are plotted. The data are normalized to the values obtained at about 20°C cold spot temperature. This value was chosen because much below 20°C the lamp operation was not steady and also the presently available information concerning isotope effects implies a negligible improvement in lamp operation at or below 20°C cold spot temperature for a F40T/12 lamp. Figures 3 and 4 show the U.V. data obtained.

GTE researchers also reported the performance of relative U.V. emission measurements from a quartz sectioned F40T/12 lamp as a function of ^{201}Hg concentration and cold spot temperature. Three capsules containing 0.30 mg ^{201}Hg were opened and mixed with the initial 3.03 mg of natural Hg. Four separate sets of data were obtained, corresponding to initial natural Hg, 0.30 mg ^{201}Hg added, 0.60 mg ^{201}Hg added and 0.90 mg ^{201}Hg added. Cold spot temperature was varied from 20°C to 45°C and U.V. output was measured. Relative to 20°C, natural Hg showed a maximum U.V. per arc watt output of 1.405 at 40°C whereas for the 0.30 and 0.60 mg of added ^{201}Hg, a maximum U.V. per arc watt output of 1.35 at 40°C was found. This decrease is not understood at this time. After the third capsule was opened, however, the maximum U.V. per arc watt output of 1.407 at 40°C was found. The estimated accuracy of these measurements was $\pm$1.0%, and they are summarized below:

Case #	Total Hg	Added Hg	Added ^{201}Hg*	Total ^{201}Hg	% ^{201}Hg	Relative UV/arc watt
1	3.03 mg	0 mg	0 mg	0.4145 mg	13.68	1.000
2	3.33	0.30	0.27	0.6845	20.56	0.961
3	3.63	0.30	0.27	0.9545	26.29	0.961
4	3.93	0.30	0.27	1.2245	31.16	1.001

*The reported istopic purity for ^{201}Hg was 90%.

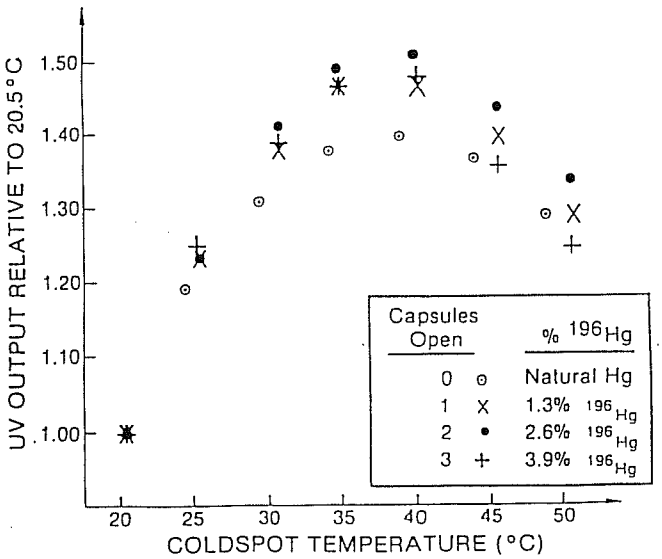

Figure 3. Variation of U.V. output (253.7nm) as a function of lamp wall temperature for different ^{196}Hg concentrations.

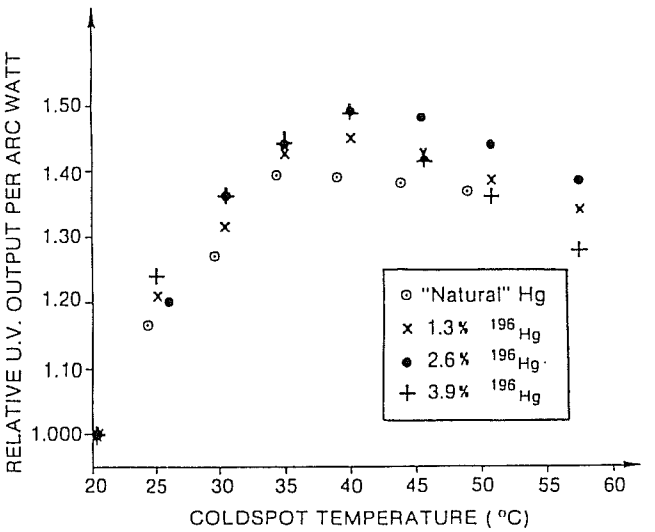

Figure 4. Variation of U.V. output (253.7nm) per arc watt as a function of lamp wall temperature for different ^{196}Hg concentrations.

Similar measurements of UV production efficiency via ^{201}Hg enrichment are being performed at LBL. These studies were inspired by the theoretical work of Richardson and Berman[12] and, while still incomplete, do provide additional encouragement toward confirming the veracity of the isotope blending efficiency enhancement process.

The LBL program is similar to that at GTE in that ampules containing ^{201}Hg are located within a discharge tube and are sequentially opened to vary the enrichment level of ^{201}Hg. Within the tube located at opposite ends behind the filaments are a pair of condensation pumps which alternately serve as the discharge tube's cold spot. When one pump is very cold, the other is kept very hot, and essentially all the discharge tube's mercury is condensed on the cold spot surface. When the other pump is suddenly activated and the formerly cold pump is simultaneously warmed, the mercury is forced to diffuse to the new cold spot surface. The total diffusion time is easily observed, and for fixed hot and cold temperatures and constant wall temperature is proportional to the total mercury mass, thus the amount of added isotope is easily observed.

The LBL preliminary results are as follows:

Case	Diffusion Time	Total Hg	^{201}Hg Mass	% ^{201}Hg	UV/Power	Relative UV/Power
1	7069	7.30 mg	0.95 mg	13%	.322	1.000
2	8758	9.10	2.56	28	.318	0.988
3	10397	11.00	4.31	39	.323	1.005
4	10867	11.49	4.71	42	.323	1.004
5	12961	13.66	6.73	49	.330	1.024
6	14544	15.22	8.16	54	.327	1.016

The greatest uncertainty in these measurements is the arc power. The lamps employed are physically short and the fraction of input power lost in the electrode fall regions is currently unknown but is assumed to be a substantial part of the total. Thus the above efficiency figures are low because they include electrode losses. It is notable that the dip in observed efficiency with low values of ^{201}Hg enrichment and the subsequent recovery with higher levels of enrichment that was reported by GTE were also observed in this study.

The magnetic enhancement of resonance radiation production efficiency is studied at LBL with the apparatus shown in Fig. (5), which consists of an integrating cylinder located within the useful volume of a pair of water cooled Helmholtz coils.

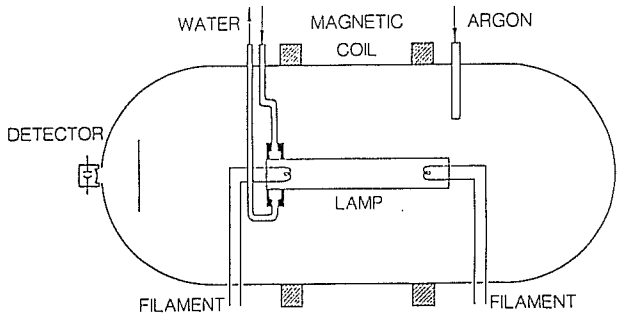

Figure 5. Zeeman effect discharge apparatus and integrating photometer.

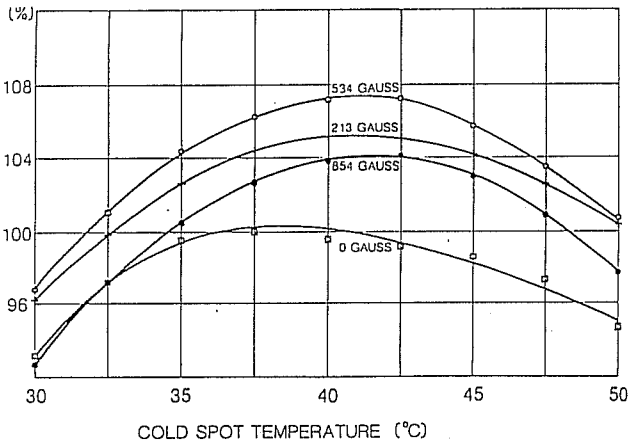

Figure 6. Relative U.V. radiation efficiency.

Provision is made for a gentle argon through flow to prevent ozone formation, and the lamp's cold spot temperature is externally controlled. It has been found that, for the case of a T/12 discharge tube with the arc totally immersed in the axial magnetic field, the UV radiation production efficiency increases with increasing uniform magnetic field for fields less than about 530 gauss. A peak efficiency enhancement of about 7% is observed at 530 gauss, and with larger values of magnetic field the efficiency decreases. The cold-spot temperature dependence of this phenomenon is shown in Fig. (6), where the shifting of the temperature of maximum efficiency to higher values with increasing magnetic field strength is clearly demonstrated. The effects on the hfs of the applied magnetic field are shown in Fig. (7).

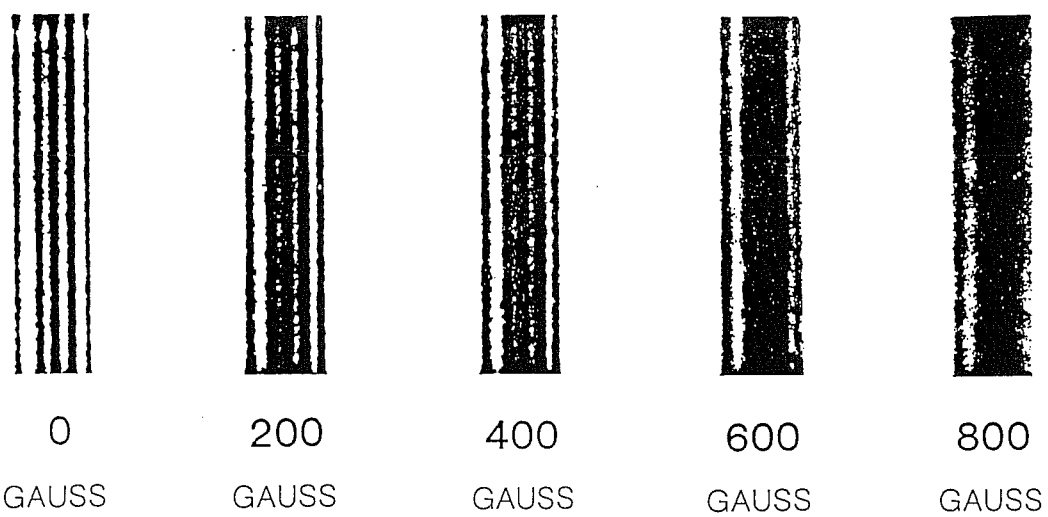

Figure 7. Hyperfine structure of λ2537 in magnetic field.

Supplementary observations were made of the effects of the external magnetic field on the UV emittances of discharge tubes of lesser diameter. It was found that a relatively strong dependence on discharge tube diameter appeared to govern the magnetic field versus emittance relationship. This is shown in Fig.(8)where the relative UV emittance of tubes of 5/8", 1" and 1-1/2" are presented as a function of applied magnetic field.

GTE also has investigated[13] the effects of magnetic fields on lamp efficiency, observing both UV at λ2537 and emission from phosphor coated lamps. Their study included both local and integrating sphere measurements employing axial and transverse magnetic fields.

The integrating sphere measurements permit measurement of light emitted over 4 π steradians from the entire lamp surface. The GTE integrating sphere measurements are summarized below:

Test No.	Lamp	Field Configuration	Field Strength	LPW Increase	Field Generation
1	F40T/12	Transverse	40G	2.2%	Permanent Magnet Strips
2	F40T/12	Transverse	110G	4%	Permanent Magnet Strips
3	F40T/12	Axial	275G	1%	Permanent Ring Magnets
4	G8T/5	Axial	0-400G	(10%)*	2 Helmholtz Coils Center
5	Bent T/5	Transverse	100G	6%	Bar magnets
6	F20T/12	Axial	0-100G	5%	7 Helmholtz coils

*253.7nm output/lamp watt increase.

Advances in HID lighting - the electrodeless lamp

An inductively coupled, high-pressure electrodeless arc[14] is an attractive HID development source[15,16] because, in the absence of electrodes, practically any candidate discharge/illumination material that can be vaporized can also be evaluated as a light source. In its usual configuration the electrodeless arc is formed when azimuthal currents are induced in a discharge tube mounted axially in an induction coil. The resulting discharge effectively forms a one-turn secondary winding of the induction coil. If the coil and its plasma contents are considered as a two port circuit element carrying current I with V input volts and P input power, the relative voltage-current phase angle is $\theta = \cos^{-1}(P/VI)$ and

$$X = Z \sin \theta$$
$$R = Z \cos \theta,$$

where Z = V/I. Thus, the electrodeless arc can be completely characterized electrically in terms of its induction coil by means of the direct measurements of the voltage across the induction coil, the current through it, and the total dissipation.

A simple discharge-producing apparatus for laboratory use is diagrammed in Fig. (9). The discharge is often formed in a 38 mm diameter quartz sphere in which mercury is added for pressure stabilization after discharge ignition. Metallic halides are dispensed in prescribed amounts and the bulb is backfilled with several- to several tens- torr of an inert gas prior to tipoff.

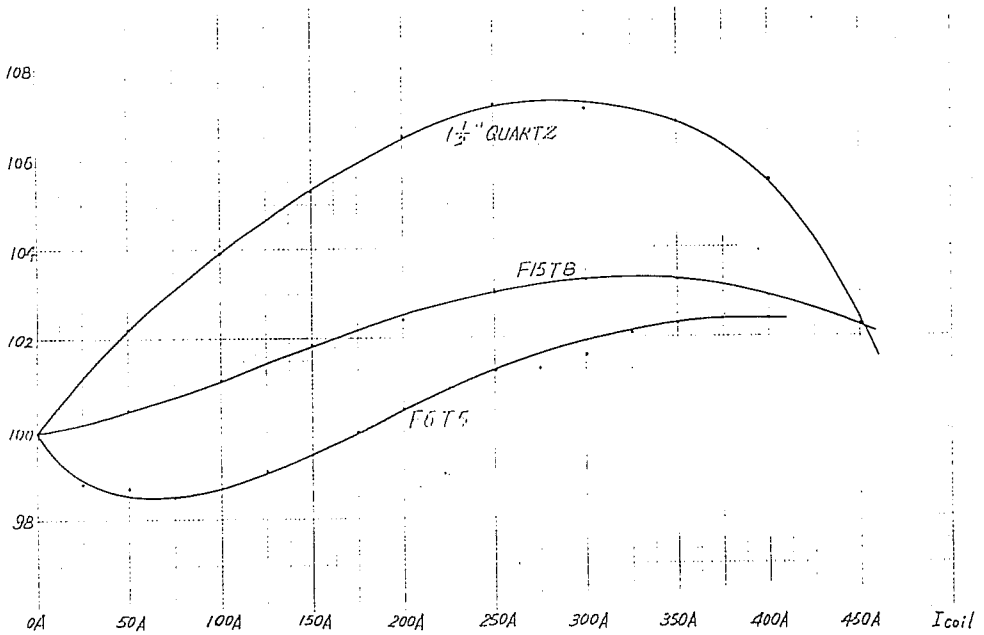

Figure 8. Relative efficacies of several commercial fluorescent lamps of varying diameter in a magnetic field.

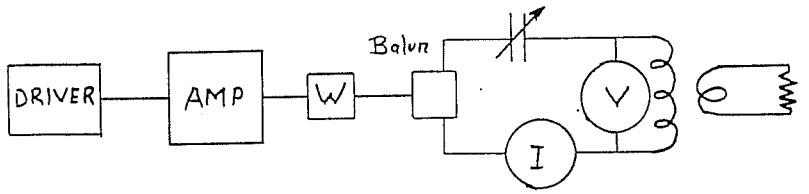

Figure 9. Electrodeless discharge apparatus.

A modular MOPA (master oscillator-power amplifier) system is shown in Fig. (9). A rugged amplifier, which can withstand large reflected powers during periods of impedance mismatch is believed essential. An in-line wattmeter is preferred for the incident minus reflected power measurement and a high power balun transformer couples the unbalanced line to the balanced load. A series resonant tuned circuit insures that this load appears resistive and also provides for Q-multiplication of coil voltage[19] to facilitate initial lamp breakdown.

Under subcontract to LBL, General Electric Co. has employed an electrodeless arc[17] to evaluate certain metallic halides[18] which would otherwise react with electrode materials. According to GE, in the selection of arc ingredients for electrodeless HID lamps, an important consideration is the energy level structure of the radiative species. The perfect level structure should be a two level system with transition energy in the range of 1.75 to 3 ev which corresponds to the energy of the visible photon. The ionization energy should be low enough only to provide enough electrons and ions to sustain a stable discharge at the required conditions of temperature and pressure. Sodium is an outstanding radiative atomic specie. Thallium is also a radiative atomic specie candidate. In addition, rare-earth atoms, for example, cerium, holmium and dysposium, have nearly ideal energy level structures. These atoms have thick forest-like spectral lines throughout the whole visible range. However, they lose some energy in UV regions by ionic radiation. Fortunately, this can be overcome in part by introducing cesium, which has very low ionization energy, to lower the plasma temperature.

Chemically, there are several important criteria in the selection of arc ingredients for electrodeless HID lamps. The first is chemical reaction with fused quartz, which has been selected as the envelope material. The electrodeless operating mode broadens the choice of arc ingredients to include the chlorides and bromides of many elements. The second important chemical criteria is any molecular specie which dissociates during arc operation must recombine in the cooler regions of the arc tube, or when the lamp is turned off. With some rare earth iodides, dissociation occurs, leaving metal atoms at the arc tube wall which attach to or devitrify the fused quartz. Since the dissociation energies of chlorides and bromides are generally higher than those of the iodides, deterioration of arc tubes should be reduced by using chlorides or bromides. Another important requirement is the metal halide should provide a sufficient vapor pressure at the operating temperature of a quartz tube. An important mechanism for enhancing the vapor density of radiating species is the formation of sodium complexes which have higher vapor pressure than simple sodium halides.

Guided by these considerations, about twenty lamps with different ingredients were examined by General Electric. The electrical and optical parameters of some typical lamps, as well as their ingredients, are listed in Table II. Data of a commercial HID lamp are included (No. 8 and No. 9) for comparison.

The efficacy of the No. 1 lamp was only about 79lm/w because of the large amount of UV radiation. The No. 2 lamp has a high efficacy because Yb is strong in the visible and very weak in the IR. Sodium also made a significant contribution to the Na-D line region. The No. 3 and No. 4 lamps have the same radiative species which have been known to give very high efficacy and good color. Bromides were used in the No. 4 lamp and it had a higher vapor pressure and higher efficacy than in the No. 3 lamp in which chlorides were used. The efficacy of 171 lm/w with a CRI of 52 has not previously been observed to our knowledge. In the No. 5 and No. lamps an attempt was made to incorporate some tin halide and sodium complexes. Due to the presence of broad continuum spectra, the No. 5 lamp has a higher CRI value. Although the No. 5 and No. 6 lamps were not as good as the No. 4 lamp, they were much better than the commercial lamp (No. 8). The output of the No. 7 lamp was dominated by molecular radiation, though it wasted very little energy in the IR and had substantial output in the UV. This is why the lamp efficacy is 60-70 lm/w. Generally, discharges dominated by molecular radiation have lower efficacy than those with strong atomic radiation.

Table II

Lamp	Composition	P(w)	E(V/am)	F(lm)	(lm/w)	CRI
1	Hg, $HgCl_2$	757.3	10.8	60099	79	--
2	Hg, $HgCl_2$, NaCl, Yb	1248.3	15.1	192194	154	--
3	Hg, TlCl, $CeCl_3$, NaCl	1262.7	17.2	184234	146	--
4	Hg, TlBr, $CeCl_3$, NaBr	1215.9	14.3	207842	171	52
5	Hg, $HgBr_2$, NaBr, TlBr, Sn, $CeCl_3$	1152.4	16.6	174063	151	60
6	Hg, $HgBr_2$, NaBr, TlBr, Yb, Sn	1193.1	16.4	186549	156	50
7	Hg, $HgCl_2$, Sn	530.0	17.9	35135	66	--
8	Commercial Metal Halide Lamp	1000.0	--	88000	88	50
9	Commercial High Pressure Sodium Lamp	1000.0	--	126000	126	25

Summary

It has only been the recent concern due to the increasing cost of electric energy that fundamental research on light sources has been renewed. This paper has reviewed some of the current work that is studying the loss processes in transforming electrical energy into visible light. The results clearly show significant improvements in efficacy of gas discharge light sources can be realized. These goals can be achieved by a better understanding of the physical processes and in their application.

References

1. P. van de Weijer and R.M.M. Cremers, J. Appl. Phys. 57(3), 672 (1985).
2. R.W. Wood, Phil. Mag. 23, 689 (1912).
3. D. Alpert, A. McDoubry, and T. Holstein, Phys. Rev. 76, 1257 (1949).
4. T. Holstein, Phys. Rev. 72, 1212 (1947).
5. T. Holstein, Phys. Rev. 83, 1159 (1951).
6. L.M. Bieberman, JETP 17, 416 (1947).
7. A.C.G. Mitchell and M.W. Zemansky, Resonance Radiation and Exited Atoms, Cambridge University Press (1934), Chapter 1.
8. M. W Zemansky, Phys. rev. 29, 513 (1927).
9. L. Hayner, Phys. Rev. 26, 364 (1925).
10. T. Holstein, et al., Phys. Rev. 85, 985 (1952).
11. S.G. Johnson, D.E. Work, J. Maya and J.F. Waymouth, Proc. of 3rd Int. Symp. on the Science and Technology of Light Sources, Toulouse, France, April (1983).
12. R.W. Richardson and S.M. Berman, Proc. of 3rd Int. Symp. on the Science and Technology of Light Sources, Toulouse, France, April (1983).
13. J. Maya, et al., Test, Evaluation, and Report on Mercury Enrichment for Fluorescent Lamps, Annual report for Subcontract No. 4524210, Lighting Systems Research, Lawrence Berkeley Laboratory, University of California, Berkeley, CA 94720, November (1985).
14. H.U. Eckert, The Induction Arc: A State of the Art Review, High Temperature Science 6, 99-134 (1974).
15. D.D. Hollister, High Pressure Method for Producing an Electrodeless Plasma Arc as a Light Source, U.S Patent no. 3,763,392 (1973).
16. D.D. Hollister, Method for Using Metallic Halides for Light Production in Electrodeless Lamps, U.S. Patent No. 3,860,854 (1975).
17. J.M. Anderson, et al., Electrodeless HID Lamp Study, Final Report under subcontract 4522010, Lawrence Berkeley Laboratory, University of California, Berkeley, CA 94720, April 1 (1984).
18. J.M. Anderson, et al., New Arc Ingredients for HID Lamps, Final Report under DOE #DE-AC0376SF00098 , LBL, University of California Berkeley, CA 94720, July 1 (1985).
19. F. Langford-Smith, Editor, Radiotron Designers Handbook, Radio Corporation of America, Harrison, NJ, Ed. 4, pg. 409 (1952).